

# Enantioselective synthesis of *N*-alkylindoles enabled by nickel-catalyzed C–C coupling

Received: 19 June 2022

Accepted: 28 October 2022

Published online: 11 November 2022

Lun Li<sup>1,3</sup>, Jiangtao Ren<sup>1,2,3</sup>, Jingjie Zhou<sup>1</sup>, Xiaomei Wu<sup>1</sup>, Zhihui Shao<sup>1,2</sup>✉, Xiaodong Yang<sup>1</sup>✉ & Deyun Qian<sup>1</sup>✉

Enantioenriched *N*-alkylindole compounds, in which nitrogen is bound to a stereogenic sp<sup>3</sup> carbon, are an important entity of target molecules in the fields of biological, medicinal, and organic chemistry. Despite considerable efforts aimed at inventing methods for stereoselective indole functionalization, straightforward access to a diverse range of chiral *N*-alkylindoles in an intermolecular catalytic fashion from readily available indole substrates remains an ongoing challenge. In sharp contrast to existing C–N bond-forming strategies, here, we describe a modular nickel-catalyzed C–C coupling protocol that couples a broad array of *N*-indolyl-substituted alkenes with aryl/alkenyl/alkynyl bromides to produce chiral *N*-alkylindole adducts in single regioisomeric form, in up to 91% yield and 97% ee. The process is amenable to proceed under mild conditions and exhibit broad scope and high functional group compatibility. Utility is highlighted through late-stage functionalization of natural products and drug molecules, preparation of chiral building blocks.

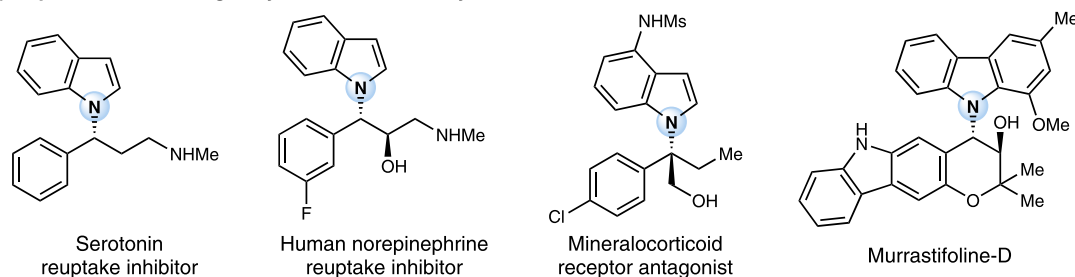
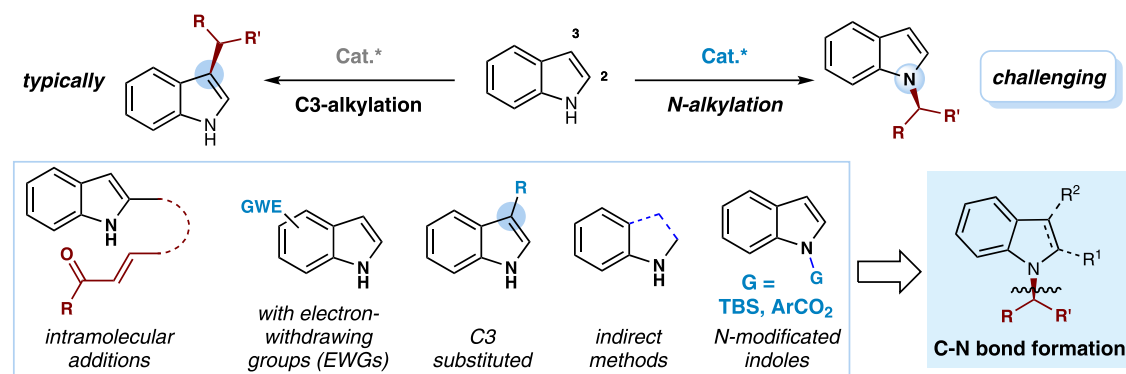
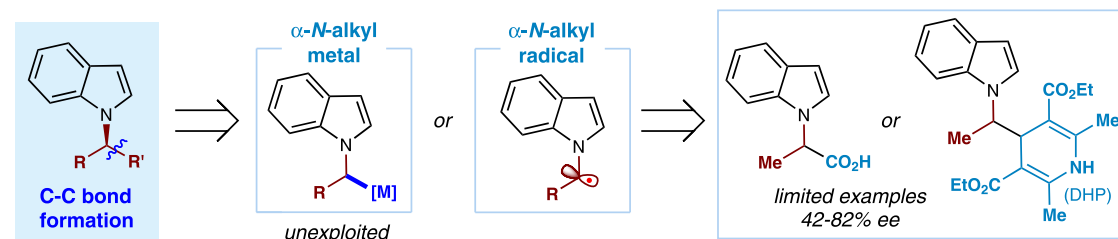
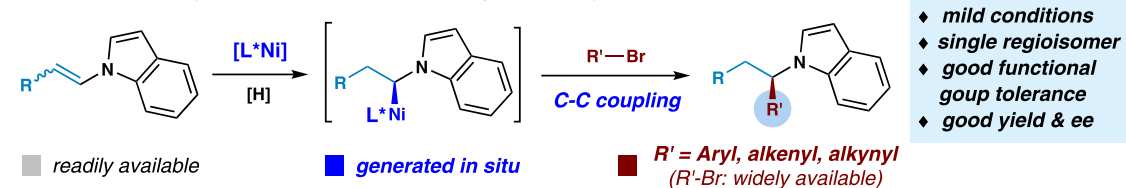
Enantioenriched indole derivatives are of great interest in pharmaceutical science and organic chemistry<sup>1–4</sup>. Particularly, the indole core is one of the most frequent *N*-heterocyclic fragment featured in FDA-approved drugs<sup>5</sup>. Therefore, different methods have been designed for the construction of chiral indole scaffolds<sup>6–9</sup>. The most typical functionalizations of indoles take place at the C3 positions, due to their innate nucleophilicity<sup>10,11</sup>. In contrast, the development of techniques involving a stereocenter adjacent to the nitrogen, an essential structural motif imbedded in many biologically active molecules (Fig. 1A)<sup>12–16</sup>, remains a great challenge, presumably owing to the attenuated nucleophilicity of the nitrogen atom (Fig. 1B). To this end, a few powerful C–N bond-forming approaches have been developed to access chiral *N*-alkylindoles (Fig. 1B). However, these transformations often rely on the enantioselective intramolecular addition of prefunctionalized indole substrates<sup>17–19</sup>, or intermolecular *N*-alkylation (mostly *N*-allylation) of indoles with C3-blocking substituents<sup>20–25</sup> or electron-withdrawing groups<sup>26–33</sup>. Moreover, indirect methods using indole precursors such as indolines or aryl hydrazines were also developed to obtain high regio- and enantioselectivity<sup>34–36</sup>. Recently,

the Vilotijevic and Buchwald groups demonstrated elegant works using *N*-modified strategy to engage *N*-silyl indoles and *N*-(benzoyloxy)indoles in C–N bond-forming reactions, respectively<sup>37,38</sup>. Despite these remarkable advances, a general, modular and selective synthesis of enantioenriched *N*-alkylindoles is in crucial demand, particularly if the substrates and catalysts are readily available<sup>39,40</sup>.

New strategic bond-forming reactions would offer a complementary protocol to existing C–N bond-forming process and an opportunity to explore currently inaccessible chemical space. In this regard, the enantioselective coupling of an  $\alpha$ -*N*-alkyl metal species or an  $\alpha$ -*N*-alkyl radical species represents a straightforward strategy to the synthesis of chiral alkyindoles (Fig. 1C)<sup>41,42</sup>. However, forging a C–C bond asymmetrically at the position  $\alpha$  to the indole nitrogen remains elusive<sup>43–45</sup>. Recently, the Melchiorre<sup>43</sup> and Davidson<sup>44</sup> groups independently reported impressive works using photoredox chemistry to engage indole-derived  $\alpha$ -*N*-alkyl radical intermediates in *N*-alkylindole synthesis, despite limited substrate scope and enantioselectivity (Fig. 1C, right). Moreover, in the the case, a leaving group (–CO<sub>2</sub>H or DHP) is necessary for the generation of an  $\alpha$ -*N*-alkyl radical. In contrast,

<sup>1</sup>Key Laboratory of Medicinal Chemistry for Natural Resource, Ministry of Education, School of Chemical Science and Technology, Yunnan Provincial Center for Research & Development of Natural Products, and State Key Laboratory for Conservation and Utilization of Bio-Resources in Yunnan, Yunnan University, Kunming, China. <sup>2</sup>Southwest United Graduate School, Kunming, China. <sup>3</sup>These authors contributed equally: Lun Li, Jiangtao Ren.

✉ e-mail: [zhihui\\_shao@hotmail.com](mailto:zhihui_shao@hotmail.com); [xyang@ynu.edu.cn](mailto:xyang@ynu.edu.cn); [dyqian@ynu.edu.cn](mailto:dyqian@ynu.edu.cn)

A) Representative biologically active chiral *N*-alkylindole derivativesB) Existing C-N bond-forming methods to access chiral *N*-alkylindole derivativesC) C-C bond-forming strategy to access chiral *N*-alkylindole derivativesD) This work: catalytic, modular, unified coupling of  $\alpha$ -*N*-alkyl-Ni species

**Fig. 1** | Representative chiral *N*-alkylindole derivatives and strategies for catalytic enantioselective synthesis of *N*-alkylindoles. **A** Representative biologically active chiral *N*-alkylindole derivatives; **B** Existing C-N bond-forming methods to

access chiral *N*-alkylindole derivatives; **C** C-C bond-forming strategy to access chiral *N*-alkylindole derivatives; **D** This work: catalytic, modular, unified coupling of  $\alpha$ -*N*-alkyl-Ni species.

there have been no reports on generation and coupling of indole-derived  $\alpha$ -*N*-alkyl metal species. The enantioselective Ni-catalyzed reductive coupling of olefins with electrophiles represents an attractive utilization of in-situ generated alkyl-Ni species<sup>46-52</sup>. We wondered whether this reductive coupling strategy could be harness to access chiral *N*-alkylindoles. However, catalytic enantioselective reductive coupling of *N*-alkenyl indoles faces several challenges. First, current asymmetric reductive coupling is largely limited to the use of linear alkyl-Ni intermediates<sup>46-58</sup>. Catalytic enantioselective coupling of branched alkyl-Ni intermediates generated from hydronickellation of olefins remains elusive<sup>59-63</sup>. Moreover, modulation of the site-selectivity pattern across differently substituted *N*-alkenyl indoles is unknown. In addition, the propensity of *N*-alkenyl polymerization and reduction is possible<sup>64-67</sup>.

As a part of our interest in chiral alkylamine-bearing molecules<sup>25,68</sup>, here, we show a catalytic enantioselective coupling of in-situ generated  $\alpha$ -*N*-alkyl nickel species with aryl/alkenyl/alkynyl bromides, analogous to the C(sp<sup>3</sup>)-C(sp<sup>2</sup>)/C(sp) cross-coupling reaction, enabling a unified method toward structurally diverse chiral *N*-alkylindoles in high yields and ee's (Fig. 1D). By employing mild conditions, this modular, unified fragment coupling provides practical advantages in reaction efficiency, functional group compatibility, as well as substrate availability and scope, which would be broadly useful yet mechanistically orthogonal to established *N*-alkylation processes. In particular, application in late-stage diversification of many natural products and drug molecules demonstrates its utility in accelerating access to *N*-alkylated drug-like complexity.

**Table 1 | Summary of the effects of crucial reaction parameters<sup>a</sup>**

Reaction scheme:  $1a + Ar-Br (2a, 2.0 \text{ eq.}) \xrightarrow[NiCl_2 \cdot DME (10 \text{ mol\%}), L^* (15 \text{ mol\%})]{(OEt)_2MeSiH/KF (1.2/1.5 \text{ eq.}), \text{Dioxane (0.2 M), } 40^\circ C, 20 \text{ h}}$   $3a$

Ligand structures and substituents:

- $R' = Me$
- $R = Ph$ ,  $L^*1$
- $R = Bn$ ,  $L^*2$
- $R = i-Pr$ ,  $L^*3$
- $R = t-Bu$ ,  $L^*4$
- $R' = H$
- $R = Ph$ ,  $L^*5$

Entry	Variant	Yield (%)	ee (%) <sup>b</sup>
1	$L^* = L^*1$	36	79
2	$L^* = L^*2, L^*3, L^*4, \text{ or } L^*5$	trace	n.d.
3	$L^* = L^*6$	34	16
4	$L^* = L^*7$	62	58
5	$L^* = L^*1$ , DME as solvent, rt	80	81
6	$L^* = L^*1$ , DCE as solvent, rt	16	88
7	$L^* = L^*1$ , DME/DCE (3:1) as solvent, rt	82	86
8	NiBr <sub>2</sub> ·DME as Ni-Cat. vs. entry 7	78	88
9	NiI <sub>2</sub> ·xH <sub>2</sub> O as Ni-Cat. vs. entry 7	81 (77) <sup>c</sup>	92

<sup>a</sup>See the SI for experimental details; all reactions were carried out in 0.2 mmol scale with respect to **1a**; corrected <sup>1</sup>H NMR yields using CH<sub>2</sub>Br<sub>2</sub> as an internal standard were reported. <sup>b</sup>The enantiomeric excesses (ee's) were determined by HPLC analysis. <sup>c</sup>Isolated yield is shown in the parenthesis.  $L^*$  chiral ligand; DME 1,2-dimethoxyethane; DCE 1,2-dichloroethane, rt room temperature; h hour; n.d. not detected.

## Results

### Reaction discovery and investigations

By the use of 4-bromophenylacetone as the coupling partner, we firstly examined the reaction of *N*-vinylindole **1a**, representing a class of nucleophiles that has previously been unexploited in asymmetric nickel-catalyzed reactions although has been widely utilized as monomers for the synthesis of polymeric materials<sup>64,69</sup>. Upon investigating a series of reaction parameters (Table 1 and Supplementary Tables 1–6), we discovered that running of the cross-coupling partners at 40 °C for 20 h in the presence of NiCl<sub>2</sub>·DME, commercially available (*S,S*)-diphenyl-Box ligand ( $L^*1$ ), a hydride source (diethoxy-methylsilane), and a base (KF) provides the desired product in 36% yield and 79% enantiomeric excess (ee) as a single isomer (entry 1). Compared to  $L^*1$ , employing bis-oxazoline analogs  $L^*2$ – $L^*4$  bearing alkyl substituents (*R*) almost did not produce **3a**. Moreover, the isopropylidene bridge of  $L^*1$  proved to be essential, as  $L^*5$  with *gem*-H could not afford the product. Inferior results were found with other chiral nitrogen-based ligands, such as pyridine-oxazoline (Pybox) and 2,2-bis(2-oxazoline) (Bi-Ox) ligands (entries 3–4). Further solvent screening indicated 1,2-dimethoxyethane was superior to other solvents, producing **3a** in good yield and ee under room temperature (entry 5). Interestingly, the mixed solvent (DME/DCE) turned out as the best solvent to obtain both high yield and high enantioselectivity (entries 5–7), thus indicating the subtle interplay of reagents and solvents in this case. In addition, use of other nickel salts, NiBr<sub>2</sub>·DME resulted in higher ee (entry 8), while NiI<sub>2</sub>·xH<sub>2</sub>O gave the best result (entry 9).

### Reaction scope

The generality of this catalytic enantioselective method is broad (Fig. 2). Concerning the aryl bromide, the reaction proceeded smoothly with a wide array of substrates to provide the corresponding products in moderate to high yields with universally high enantioselectivities. Notably, electron-deficient or electron-rich arenes were amenable coupling partners, in which the substituent could be placed at *para* and

*meta* position. A variety of functionalities such as a nitrile (**2b**), trifluoromethyls (**2c**, **2p**, **2r**), esters (**2d**, **2m**, **2q**), halides (**2f**, **2g**, **2n**, **2o**), ethers (**2i**, **2j**) were all readily accommodated. Despite the ability of nickel complex to activated aryl chlorides, our approach could tolerate Ar-Cl groups (**2f**, **2o**). In particular, sensitive functional groups including easily reduced ketone (**2a**) and aldehyde (**2e**), and triflate (**2k**) and boronic acid pinacol ester (**2l**) commonly used for cross-coupling, all remained intact under the standard reaction conditions. Furthermore, the pharmaceutically important heterocycle–pyridine (**2r**) was compatible as well.

Next, we sought to survey the influence of the *N*-vinylindole variants that could be used in the catalytic hydroarylation event. Delightfully, a diverse array of functional groups were suitable at different positions on the benzene ring of the indole, including a 6-methoxy (**3s**), 6-fluoro (**3t**), 6-cyano (**3u**), and 5-methyl (**3v**) substituent. It is worth noting that alkyl group at the C3-position of the indole scaffold was accommodated, delivering the corresponding product **3w** in moderate yield but with excellent enantioselectivity, which is difficult to obtain employing previous CuH catalysis<sup>38</sup>. In addition, carbazole-derived substrate afforded the desired *N*-alkylated product in moderate yield and enantioselectivity (**3x**). Gratifyingly, a diverse set of more sterically hindered (*Z*)-*N*-alkenyl indoles were also successfully transformed utilizing this method, and the corresponding *N*-alkylindoles were readily prepared in useful yields with good levels of enantioselectivity (**3y**–**3dd**). However, (*E*)-*N*-alkenyl indoles performed lower reactivity and slightly lower enantioselectivity than their *Z* isomers (e.g., **3y**: 19%, 84% ee vs. 41%, 87% ee). The isomerization of *Z*-*N*-alkenyl substrate to its *E* isomer was observed during the reaction process, and over 40% of the *E*/*Z* mixture could be recovered after the reaction (Supplementary Method 1.6). Of note, the C–C bond-forming event occurs regioselectively at the carbon  $\alpha$  to the nitrogen of indoles, even in the presence of other directing groups such as amide (**3z**–**3bb**), ester (**3cc**), and aryl (**3dd**). Especially, this modular reaction could be applied to prepare important serotonin reuptake inhibitor

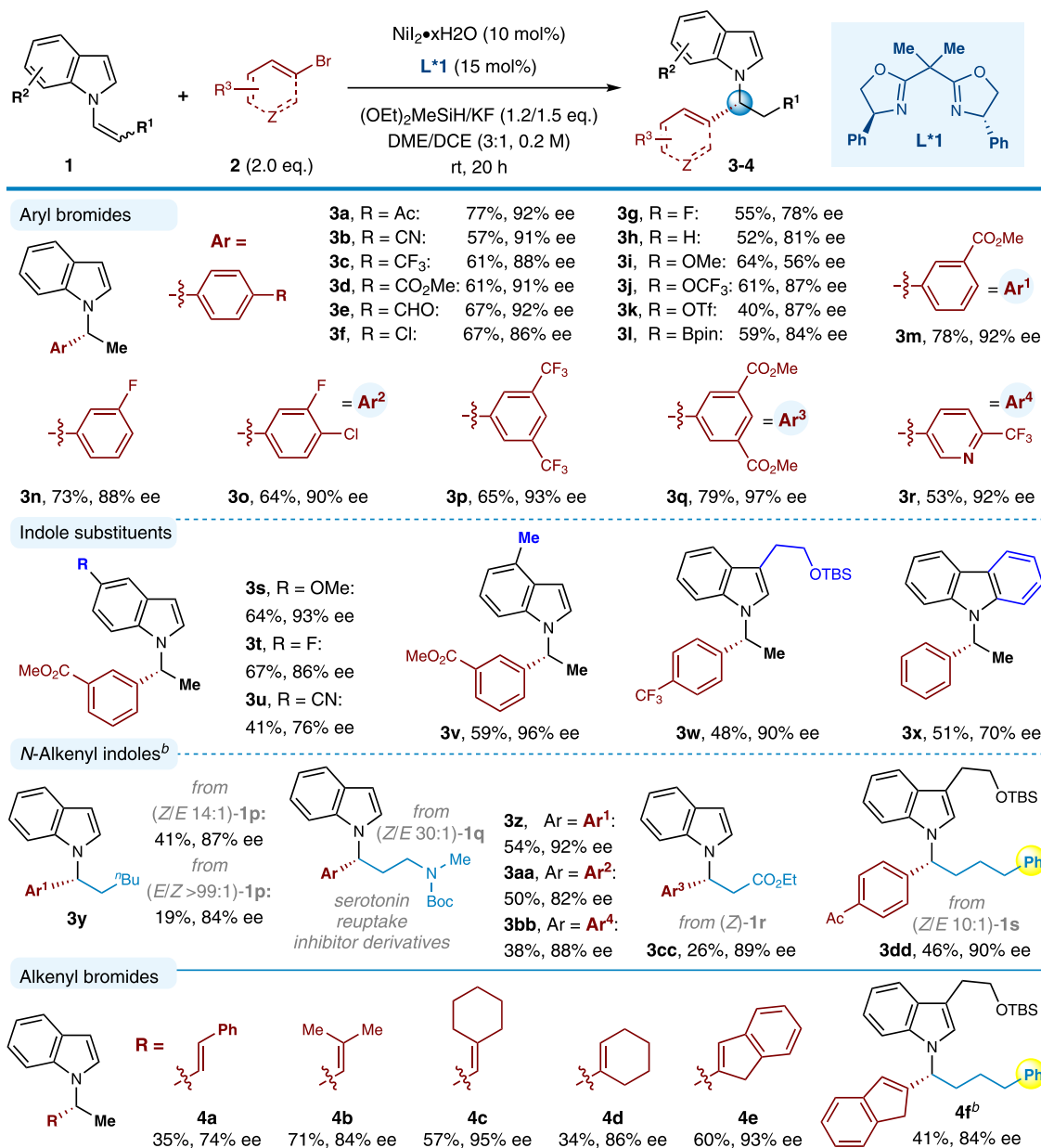


**Fig. 2 | Scope of enantioselective synthesis of *N*-benzyl and *N*-allylic indoles enabled by Ni-catalyzed C(sp<sup>3</sup>)-C(sp<sup>2</sup>) coupling reactions.** Conditions: <sup>a</sup>All reactions were carried out with Ni<sub>2</sub>·xH<sub>2</sub>O (10 mol%), ligand **L\*1** (15 mol%), **1**

(0.40 mmol), **2** (0.80 mmol), (OEt)<sub>2</sub>MeSiH (0.48 mmol), KF (0.60 mmol) and DME/DCE (3:1, 2.0 mL) at room temperature for 20 h; <sup>b</sup>DME as solvent, (OEt)<sub>2</sub>MeSiH (0.72 mmol), KF (0.88 mmol), 48 h.

derivatives with good efficiency and enantioselectivities (**3z-3bb**, 81–92% ee's).

In addition to aryl bromides, vinyl bromides were incorporated as well in this reaction, leading to structurally diverse chiral *N*-allyl indoles **4a-4f** in 35–60% yields with 73–95% ee values. Remarkably, this modular alkenylation complements previously established metal-catalyzed indole *N*-allylations in that di- and trisubstituted allylic products bearing aryl and alkyl groups are readily accessed<sup>27,29,31,70,71</sup>.

Besides the C(sp<sup>2</sup>) bromides, this catalytic C-C bond-forming reaction was also viable for C(sp) bromides–bromoalkynes **5**. While the above standard conditions with ligand **L\*1** resulted in poor enantiocontrol for the C(sp<sup>3</sup>)-C(sp) coupling (e.g., **6a**: 28% yield, 55% ee), delightfully, the reaction selectivity could be significantly improved by further optimization efforts (see Supplementary Table 7). As shown in Fig. 3, the treatment of bromoalkynes **5** and *N*-alkenylindoles **1** with 10 mol% Ni<sub>2</sub> as the catalyst, 15 mol% **L\*8** as the ligand at 0 °C could

yield the corresponding chiral *N*-propargyl indoles **6** in mostly good yields (25–89%) and high levels of enantioselectivity (ee values of 80–97%). A variety of *N*-alkenyl indoles substituted at the 4-position (**6b**), 5-position (**6c-6g**), 6-position (**6h-6j**), and 7-position (**6k, 6l**) each underwent efficient hydroalkynylation to provide the corresponding products with uniformly high enantioselectivities. Of note, alkyl group at the C3-position of the indole scaffold was demonstrated being tolerated again (**6m**). With regard to medicinal chemistry applications, the generation of product **6g** demonstrates tolerance of a pinacol boronate subunit under the conditions of catalytic enantioselective alkylation. Additionally, more sterically hindered *cis*- $\beta$ -substituted *N*-alkenyl indoles also successfully underwent C(sp<sup>3</sup>)-C(sp) bond-formation to deliver compounds **6o** and **6p**, respectively, as single regioisomers with reasonable yields and good enantioselectivities. Similar to the C(sp<sup>3</sup>)-C(sp<sup>2</sup>) coupling, the reaction reactivity and stereoselectivity was influenced by the *Z* and *E* configuration of *N*-alkenyl indoles (e.g., **6o**).



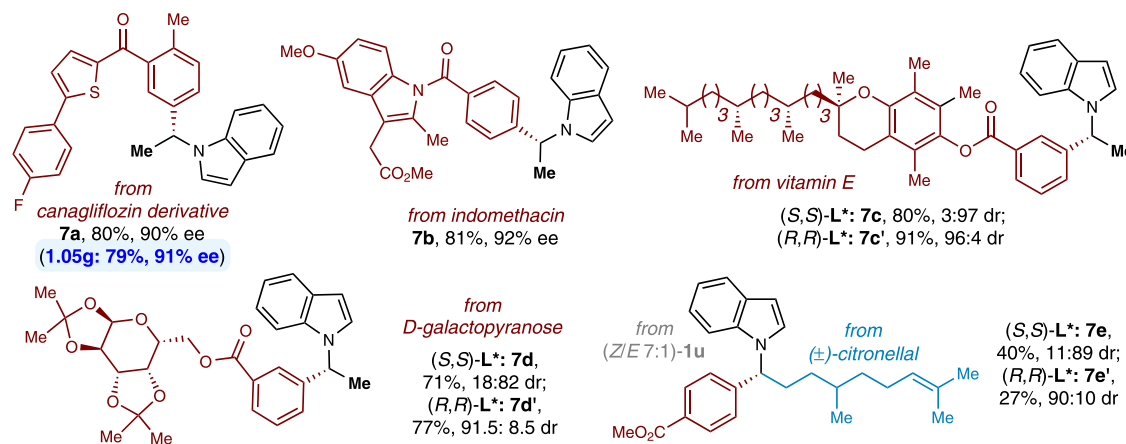


**Fig. 4 | Late-stage diversification of drug molecules and natural products.**

Conditions: All reactions were carried out with  $\text{NiI}_2 \cdot x\text{H}_2\text{O}$  (10 mol%), ligand **L1** (15 mol%), **1a** or citronellal-derived **1u** (0.40 mmol), drugs- or natural products-

derived **2** (0.80 mmol),  $(\text{OEt})_2\text{MeSiH}$  (0.48 or 0.72 mmol), KF (0.60 or 0.88 mmol) and DME/DCE (3:1, 2.0 mL) at room temperature for 20 or 48 h.

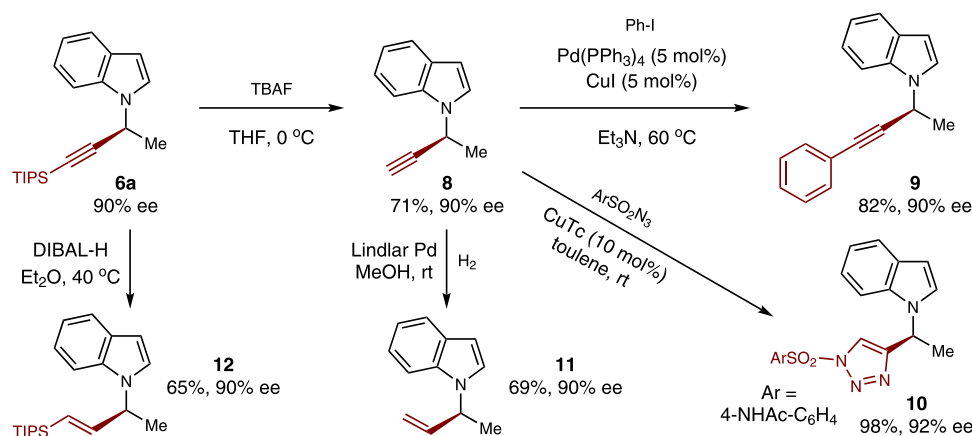


**Fig. 5 | Derivatizations of chiral *N*-propargyl indoles.** Desilylation and alkynyl reduction of compound **6a**; Sonogashira coupling, [3 + 2] cycloaddition, and hydrogenation of compound **8**. DIBAL-H = diisobutylaluminum hydride; Lindlar Pd = Pd/BaSO<sub>4</sub>; CuTc = copper(I) thiophene-2-carboxylate.

process consists of  $\pi$ -bond insertion into  $\text{L}^*\text{Ni-H}$  species, oxidative addition of the resulting  $\text{L}^*\text{Ni-alkyl}$  intermediate, and reductive elimination to form product and the  $\text{L}^*\text{Ni-H}$  catalyst<sup>46–63</sup>. Take the reductive coupling of *N*-alkenyl indoles with aryl halides as an example, competition experiments were performed to compare the reactivity between different aryl halides, indicating that (i) electron-deficient aryl bromide is more reactive than an electron-rich one (Fig. 6a–i), and (ii) aryl bromide is more reactive than aryl iodide (Fig. 6a–ii). In fact, a competing reductive hydrodehalogenation event was observed when an aryl iodide was used as the electrophile (Fig. 6a–iii)<sup>73,74</sup>, suggesting it is disadvantaged for the final product formation that oxidative addition of  $\text{L}^*\text{Ni}$  complex prior to generation of  $\text{L}^*\text{Ni-alkyl}$  intermediate. Next, the reductive coupling of **1a** was chosen for kinetic studies, and the reaction progress was monitored by <sup>19</sup>F and <sup>1</sup>H NMR. Initial rate experiments disclosed that the reaction was zero-order in *N*-alkenyl indole, first-order in catalyst and aryl bromide, and fractional-order in diethoxymethylsilane (Fig. 6b, see also Supplementary Method 1.9.1). Moreover, Hammett studies were also performed to evaluate the influence that electronic variation of the aryl electrophiles had on the rate of hydroarylation (Fig. 6c)<sup>75,76</sup>. As a result, a variety of *para*-substituted aryl bromides reacted with *N*-vinylindole **1a** at different rates, indicating that electronic variation of the aryl electrophile had a remarkable impact on the rate of *N*-vinylindole hydroarylation. A linear relationship was further observed through a Hammett plot. The positive slope ( $\rho = 0.67$ ) suggests negative charge accumulation in the turnover-determining transition state, which is stabilized by electron-

withdrawing substituents. Taken together, the above results reveal that oxidative addition is most likely the turnover-limiting step.

Furthermore, a linear correlation was observed by nonlinear effect studies on the enantiomeric composition of chiral ligand **L1** and *N*-alkylindole product **3o** (Fig. 7a), which is consistent with a ligated nickel catalyst being of a monomeric nature. To identify the enantio-determining step of the *N*-vinylindole hydroarylation reaction, we next investigated linear free energy relationships (LFERs) between the Hammett electronic parameters of various *para*-substituted aryl bromides and the enantioselectivities of the corresponding products (Fig. 7b)<sup>77,78</sup>. A linear correlation was observed with *para*-substituted aryl bromides as enantioselectivity increased with the introduction of electron-withdrawing groups ( $\rho = 1.07$ ): 56% ee and 92% ee were observed for 4-methoxyphenyl bromide ( $\sigma = -0.27$ ) and 4-acetylphenyl bromide ( $\sigma = 0.50$ ), respectively, implying that the enantioselectivity of the process is not solely under catalyst control. In addition, the silane did essentially not affect the enantioselectivity of the reaction. On the basis of these results, oxidative addition is most likely the enantiodetermining step.

As shown in Fig. 8, a more complete description of the proposed mechanism is outlined. The *syn*-hydrometallation of an  $\text{L}^*\text{Ni-H}$  species into an *N*-alkenyl indole would form alkyl-Ni(I) species (**B**). Subsequently, the selective oxidative addition between a particular isomer of the alkyl-Ni(I) species and the bromide (**2, 5**) would ultimately generate a single alkyl-Ni(III)-R enantiomer (**C**), because this step would be both the turnover-determining step and the enantio-determining step in the

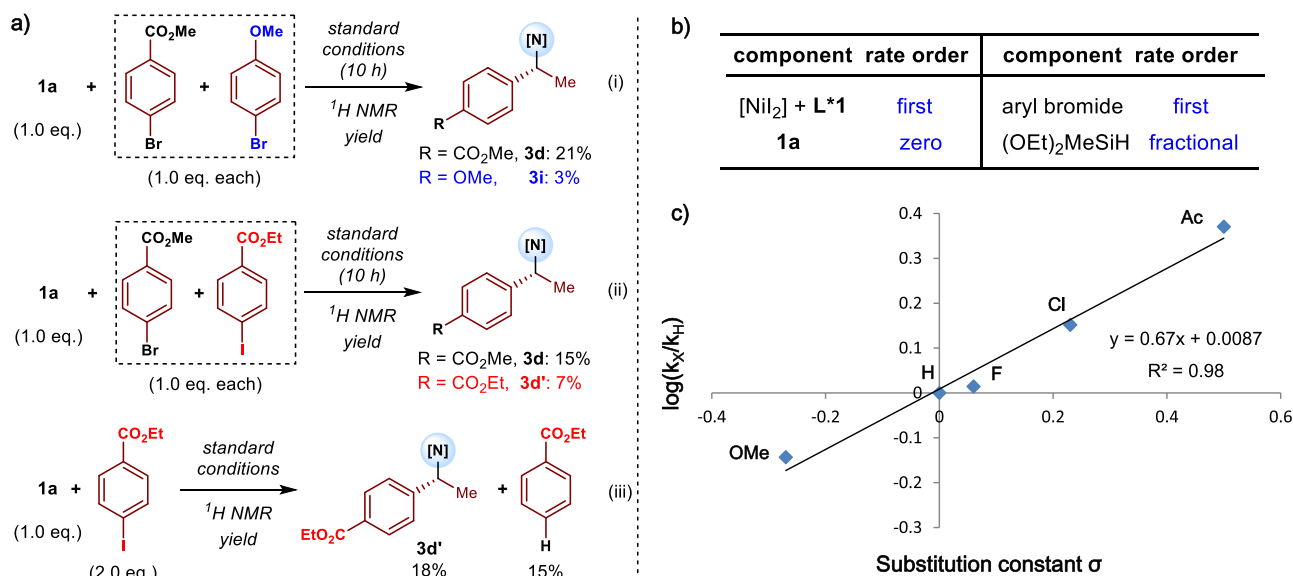


**Fig. 6 | Mechanistic experiments.** **a** Competition experiments ([N] = *N*-indolyl); **b** Initial rate experiments; **c** Hammett study for the formation of **3** versus the corresponding  $\sigma$  value ( $k$  = reaction rate).

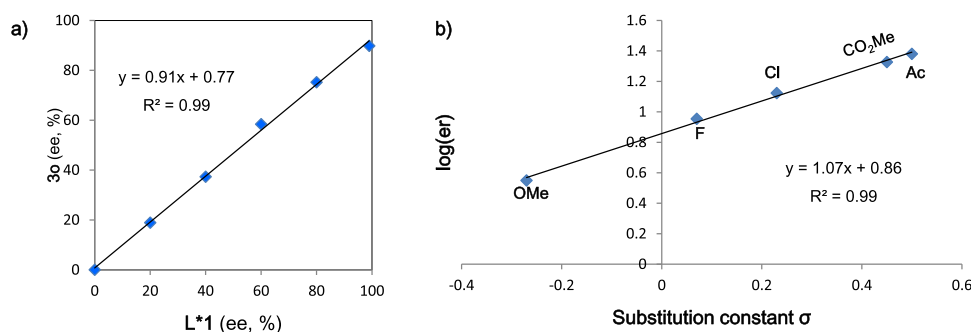


**Fig. 7 | Further mechanistic experiments.** **a** Nonlinear effect study; **b** Hammett plot for the enantiomeric ratio (er) of hydroarylation products using *para*-substituted aryl bromides.

presence of a chiral ligand (**L\*1**, **L\*8**). In particular, the favored enantioselective transition state **TS-C** would lead to the major enantiomeric product, owing to steric interactions with the ligand phenyl substituents (**TS-C'**). Then, stereospecific reductive elimination would afford the desired product (**3**, **4**, **6**, **7**) and regenerate the active nickel hydride species (**A**). Alternatively, the competitive alkyl-Ni homolysis process was also possible<sup>53,55,62,79</sup>.

In summary, we have developed a nickel-catalyzed enantioselective, modular coupling of indole-based *N*-alkyl-Ni fragments with C(sp<sup>2</sup>)/C(sp) bromides. By the use of easily accessible and stable indole-derived alkenes as nucleophiles, this protocol enables streamlined preparation of enantioenriched *N*-alkylindole molecules under mild conditions, with previously inaccessible functional group tolerance and chemical space. Application in late-stage diversification of several complex drug molecules and natural products as well as chiral syntheses demonstrates its potential utility in the synthesis of valuable chiral *N*-alkylated bioactive compounds.

## Methods

### General procedure for the enantioselective synthesis of *N*-benzyl and *N*-allylic indoles

To an oven-dried 8.0 mL Teflon-screw cap test tube containing a magnetic stir was charged with NiI<sub>2</sub>·xH<sub>2</sub>O (16.8 mg, 10 mol%) and ligand **L\*1** (20.2 mg, 15 mol%) under an N<sub>2</sub> atmosphere using glove-box

techniques. Subsequently, anhydrous DME (1.5 mL) was added, and the mixture was stirred for 15 min at room temperature. Next, KF (35.0 mg, 0.60 mmol, 1.5 equiv.), *N*-alkenyl indole **1** (0.40 mmol, 1.0 equiv.), aryl/alkenyl bromide **2** (0.80 mmol, 2.0 equiv.), DCE (0.5 mL), and (OEt)<sub>2</sub>MeSiH (78.0  $\mu$ L, 0.48 mmol, 1.2 equiv.) were sequentially added. Then the tube was sealed with airtight electrical tapes and removed from the glove box and stirred at room temperature for 20–48 h. After that, the reaction mixture was diluted with saturated NH<sub>4</sub>Cl (aq., 1.0 mL) and EtOAc (5.0 mL). The aqueous phase was extracted with EtOAc (2  $\times$  5.0 mL) and the combined organic phases were concentrated. The crude mixture was purified by flash column chromatography on silica gel using a mixture of PE/EtOAc as eluent to obtain the desired product **3**, **4**, **7**.

### General procedure for the enantioselective synthesis of *N*-propargyl indoles

To an oven-dried 12 mL Teflon-screw cap test tube containing a magnetic stir was charged with NiI<sub>2</sub> (3.1 mg, 10 mol%) and ligand **L\*8** (7.7 mg, 15 mol%) under a nitrogen N<sub>2</sub> atmosphere using glove-box techniques. Subsequently, anhydrous DME (0.25 mL) was added, and the mixture was stirred for 30 min at room temperature. Next, KF (17.4 mg, 0.30 mmol, 3.0 equiv.), *N*-alkenyl indole **1** (0.10 mmol, 1.0 equiv.), alkynyl bromide **5** (0.25 mmol, 2.5 equiv.), and (OEt)<sub>2</sub>MeSiH (43.0  $\mu$ L, 0.30 mmol, 3.0 equiv.) were sequentially added. Then the

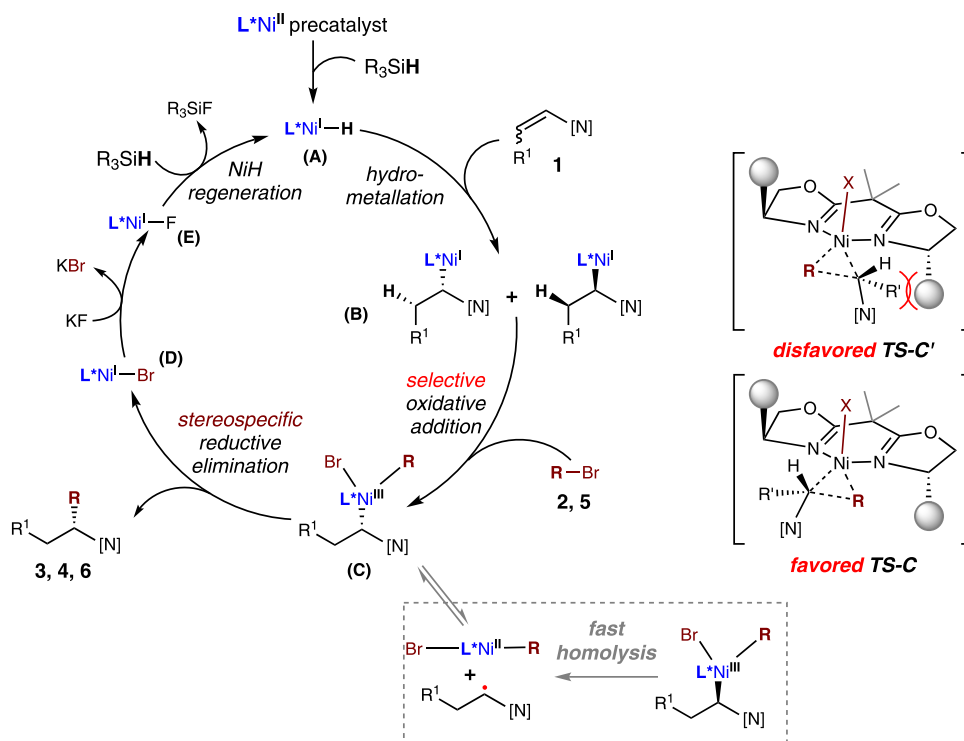


**Fig. 8 | Possible reaction pathway.** The selective oxidative addition is proposed to be both the turnover-determining step and the enantio-determining step. [N] = *N*-indolyl; TS = transition state.

tube was sealed with airtight electrical tapes and removed from the glove box and stirred at 0 °C for 36 h. After that, the reaction mixture was diluted with saturated  $NH_4Cl$  (aq., 1.0 mL) and EtOAc (5.0 mL). The aqueous phase was extracted with EtOAc ( $2 \times 5.0$  mL) and the combined organic phases were concentrated. The crude mixture was purified by flash column chromatography on silica gel using a mixture of PE/EtOAc as eluent to obtain the desired product 6.

## Data availability

The data relating to the materials and methods, experimental procedures, mechanism research, NMR spectra, and HPLC spectra are available in the Supplementary Information. All other data are available from the authors upon request.

## References

- Gul, W. & Hamann, M. T. Indole alkaloid marine natural products: an established source of cancer drug leads with considerable promise for the control of parasitic, neurological and other diseases. *Life Sci.* **78**, 442–453 (2005).
- Kochanowska-Karamyan, A. J. & Hamann, M. T. Marine indole alkaloids: potential new drug leads for the control of depression and anxiety. *Chem. Rev.* **110**, 4489–4497 (2010).
- Sravanthi, T. V. & Manju, S. L. Indoles: a promising scaffold for drug development. *Eur. J. Pharm. Sci.* **91**, 1–10 (2016).
- Singh, P. T. & Singh, M. O. Recent progress in biological activities of indole and indole alkaloids. *Mini-Rev. Med. Chem.* **18**, 9–25 (2018).
- Vitaku, E., Smith, D. T. & Njardarson, J. T. Analysis of the structural diversity, substitution patterns, and frequency of nitrogen heterocycles among U.S. FDA approved pharmaceuticals. *J. Med. Chem.* **57**, 10257–10274 (2014).
- Bandini, M. & Eichholzer, A. Catalytic functionalization of indoles in a new dimension. *Angew. Chem. Int. Ed.* **48**, 9608–9644 (2009).
- Dalpozzo, R. Strategies for the asymmetric functionalization of indoles: an update. *Chem. Soc. Rev.* **44**, 742–778 (2015).
- Trubitsön, D. & Kanger, T. Enantioselective catalytic synthesis of *N*-alkylated indoles. *Symmetry* **12**, 1184 (2020).
- Chen, J.-B. & Jia, Y.-X. Recent progress in transition-metal-catalyzed enantioselective indole functionalizations. *Org. Biomol. Chem.* **15**, 3550–3567 (2017).
- Lakhdar, S. et al. Nucleophilic reactivities of indoles. *J. Org. Chem.* **71**, 9088–9095 (2006).
- Otero, N., Mandado, M. & Mosquera, R. A. Nucleophilicity of indole derivatives: activating and deactivating effects based on proton affinities and electron density properties. *J. Phys. Chem. A* **111**, 5557–5562 (2007).
- D'Ambra, T. E. et al. Conformationally restrained analogs of pravadoline: nanomolar potent, enantioselective, (aminoalkyl)indole agonists of the cannabinoid receptor. *J. Med. Chem.* **35**, 124–135 (1992).
- Mahaney, P. E. et al. Synthesis and activity of a new class of dual acting norepinephrine and serotonin reuptake inhibitors: 3-(1*H*-indol-1-yl)-3-arylpropan-1-amines. *Biorg. Med. Chem.* **14**, 8455–8466 (2006).
- Fernandez, L. S. et al. Flindersia A–C: antimalarial bis-indole alkaloids from flindersia species. *Org. Lett.* **11**, 329–332 (2009).
- Gehling, V. S. et al. Discovery, design, and synthesis of indole-based EZH2 inhibitors. *Bioorg. Med. Chem. Lett.* **25**, 3644–3649 (2015).
- Vaswani, R. G. et al. Identification of (*R*)-*N*-((4-Methoxy-6-methyl-2-oxo-1,2-dihydropyridin-3-yl)methyl)-2-methyl-1-(1-(1-(2,2,2-trifluoroethyl)piperidin-4-yl)ethyl)-1*H*-indole-3-carboxamide (CPI-1205), a Potent and Selective Inhibitor of Histone Methyltransferase EZH2, Suitable for Phase I Clinical Trials for B-Cell Lymphomas. *J. Med. Chem.* **59**, 9928–9941 (2016).
- Bandini, M., Eichholzer, A., Tragni, M. & Umani-Ronchi, A. Enantioselective phase-transfer-catalyzed intramolecular aza-michael reaction: effective route to pyrazino-indole compounds. *Angew. Chem. Int. Ed.* **47**, 3238–3241 (2008).



18. Cai, Q., Zheng, C. & You, S.-L. Enantioselective intramolecular Aza-Michael additions of indoles catalyzed by chiral phosphoric acids. *Angew. Chem. Int. Ed.* **49**, 8666–8669 (2010).
19. Ye, K.-Y., Cheng, Q., Zhuo, C.-X., Dai, L.-X. & You, S.-L. An Iridium(II) N-heterocyclic carbene complex catalyzes asymmetric intramolecular allylic amination reactions. *Angew. Chem. Int. Ed.* **55**, 8113–8116 (2016).
20. Kainz, Q. M. et al. Asymmetric copper-catalyzed C-N cross-couplings induced by visible light. *Science* **351**, 681–684 (2016).
21. Arredondo, V., Hiew, S. C., Gutman, E. S., Premachandra, I. D. U. A. & Van Vranken, D. L. Enantioselective palladium-catalyzed carbene insertion into the N-H bonds of aromatic heterocycles. *Angew. Chem. Int. Ed.* **56**, 4156–4159 (2017).
22. Chen, M. & Sun, J. Catalytic Asymmetric N-Alkylation of Indoles and Carbazoles through 1,6-Conjugate Addition of Aza-para-quinone Methides. *Angew. Chem. Int. Ed.* **56**, 4583–4587 (2017).
23. Cai, Y., Gu, Q. & You, S.-L. Chemoselective N-H functionalization of indole derivatives via the Reissert-type reaction catalyzed by a chiral phosphoric acid. *Org. Biomol. Chem.* **16**, 6146–6154 (2018).
24. Allen, J. R., Bahamonde, A., Furukawa, Y. & Sigman, M. S. Enantioselective N-alkylation of indoles via an intermolecular Aza-Wacker-type reaction. *J. Am. Chem. Soc.* **141**, 8670–8674 (2019).
25. Wang, Y., Wang, S., Shan, W. & Shao, Z. Direct asymmetric N-propargylation of indoles and carbazoles catalyzed by lithium SPINOL phosphate. *Nat. Commun.* **11**, 226 (2020).
26. Enders, D., Wang, C. & Raabe, G. Enantioselective synthesis of 3H-Pyrrolo[1,2-a]indole-2-carbaldehydes via an organocatalytic domino Aza-Michael/Aldol condensation reaction. *Synthesis* **2009**, 4119–4124 (2009).
27. Stanley, L. M. & Hartwig, J. F. Iridium-Catalyzed Regio- and Enantioselective N-Allylation of Indoles. *Angew. Chem. Int. Ed.* **48**, 7841–7844 (2009).
28. Hong, L., Sun, W., Liu, C., Wang, L. & Wang, R. Asymmetric Organocatalytic N-Alkylation of Indole-2-carbaldehydes with  $\alpha,\beta$ -Unsaturated Aldehydes: One-Pot Synthesis of Chiral Pyrrolo[1,2-a]indole-2-carbaldehydes. *Chem. Eur. J.* **16**, 440–444 (2010).
29. Trost, B. M., Osipov, M. & Dong, G. Palladium-catalyzed dynamic kinetic asymmetric transformations of vinyl aziridines with nitrogen heterocycles: rapid access to biologically active pyrroles and indoles. *J. Am. Chem. Soc.* **132**, 15800–15807 (2010).
30. Huang, L., Wei, Y. & Shi, M. Asymmetric substitutions of O-Boc-protected Morita-Baylis-Hillman adducts with pyrrole and indole derivatives. *Org. Biomol. Chem.* **10**, 1396–1405 (2012).
31. Chen, L.-Y. et al. Enantioselective direct functionalization of indoles by Pd/sulfoxide-phosphine-catalyzed N-allylic alkylation. *Org. Lett.* **17**, 1381–1384 (2015).
32. Mukherjee, S., Shee, S., Poisson, T., Besset, T. & Biju, A. T. Enantioselective N-heterocyclic carbene-catalyzed cascade reaction for the synthesis of pyrroloquinolines via N-H functionalization of indoles. *Org. Lett.* **20**, 6998–7002 (2018).
33. Yang, X. et al. Enantioselective indole N-H functionalization enabled by addition of carbene catalyst to indole aldehyde at remote site. *ACS Catal.* **9**, 10971–10976 (2019).
34. Liu, W.-B., Zhang, X., Dai, L.-X. & You, S.-L. Asymmetric N-allylation of indoles through the iridium-catalyzed allylic alkylation/oxidation of indolines. *Angew. Chem. Int. Ed.* **51**, 5183–5187 (2012).
35. Chen, Q.-A., Chen, Z. & Dong, V. M. Rhodium-catalyzed enantioselective hydroamination of alkynes with indolines. *J. Am. Chem. Soc.* **137**, 8392–8395 (2015).
36. Xu, K., Gilles, T. & Breit, B. Asymmetric synthesis of N-allylic indoles via regio- and enantioselective allylation of aryl hydrazines. *Nat. Commun.* **6**, 7616 (2015).
37. Zi, Y., Lange, M., Schultz, C. & Vilotijevic, I. Latent nucleophiles in Lewis base catalyzed enantioselective N-allylations of N-heterocycles. *Angew. Chem. Int. Ed.* **58**, 10727–10731 (2019).
38. Ye, Y., Kim, S.-T., Jeong, J., Baik, M.-H. & Buchwald, S. L. CuH-catalyzed enantioselective alkylation of indole derivatives with ligand-controlled regioselectivity. *J. Am. Chem. Soc.* **141**, 3901–3909 (2019).
39. Sevov, C. S., Zhou, J. & Hartwig, J. F. Iridium-catalyzed, intermolecular hydroamination of unactivated alkenes with indoles. *J. Am. Chem. Soc.* **136**, 3200–3207 (2014).
40. Bartoszewicz, A., Matier, C. D. & Fu, G. C. Enantioconvergent alkylations of amines by alkyl electrophiles: copper-catalyzed nucleophilic substitutions of racemic  $\alpha$ -halolactams by indoles. *J. Am. Chem. Soc.* **141**, 14864–14869 (2019).
41. Cherney, A. H., Kadunce, N. T. & Reisman, S. E. Enantioselective and enantiospecific transition-metal-catalyzed cross-coupling reactions of organometallic reagents to construct C–C bonds. *Chem. Rev.* **115**, 9587–9652 (2015).
42. Choi, J. & Fu, G. C. Transition metal-catalyzed alkyl-alkyl bond formation: another dimension in cross-coupling chemistry. *Science* **356**, eaaf7230 (2017).
43. Gandolfo, E., Tang, X., Raha Roy, S. & Melchiorre, P. Photochemical asymmetric nickel-catalyzed acyl cross-coupling. *Angew. Chem. Int. Ed.* **58**, 16854–16858 (2019).
44. Pezzetta, C., Bonifazi, D. & Davidson, R. W. M. Enantioselective synthesis of N-benzylic heterocycles: a nickel and photoredox dual catalysis approach. *Org. Lett.* **21**, 8957–8961 (2019).
45. Lavernhe, R., Alexy, E. J., Zhang, H. & Stoltz, B. M. Palladium-catalyzed enantioselective decarboxylative allylic alkylation of acyclic  $\alpha$ -N-pyrrolyl/indolyl ketones. *Org. Lett.* **22**, 4272–4275 (2020).
46. Wang, Z., Yin, H. & Fu, G. C. Catalytic enantioconvergent coupling of secondary and tertiary electrophiles with olefins. *Nature* **563**, 379–383 (2018).
47. Zhou, F., Zhang, Y., Xu, X. & Zhu, S. NiH-catalyzed remote asymmetric hydroalkylation of alkenes with racemic  $\alpha$ -bromo amides. *Angew. Chem. Int. Ed.* **58**, 1754–1758 (2019).
48. He, S.-J. et al. Nickel-catalyzed enantioconvergent reductive hydroalkylation of olefins with  $\alpha$ -heteroatom phosphorus or sulfur alkyl electrophiles. *J. Am. Chem. Soc.* **142**, 214–221 (2020).
49. Bera, S., Mao, R. & Hu, X. Enantioselective  $C(sp^3)$ – $C(sp^3)$  cross-coupling of non-activated alkyl electrophiles via nickel hydride catalysis. *Nat. Chem.* **13**, 270–277 (2021).
50. Wang, X.-X., Lu, X., Li, Y., Wang, J.-W. & Fu, Y. Recent advances in nickel-catalyzed reductive hydroalkylation and hydroarylation of electronically unbiased alkenes. *Sci. China Chem.* **63**, 1586–1600 (2020).
51. He, Y., Chen, J., Jiang, X. & Zhu, S. Enantioselective NiH-catalyzed reductive hydrofunctionalization of alkenes. *Chin. J. Chem.* **40**, 651–661 (2022).
52. Zhang, Z., Bera, S., Fan, C. & Hu, X. Streamlined alkylation via nickel-hydride-catalyzed hydrocarbonation of alkenes. *J. Am. Chem. Soc.* **144**, 7015–7029 (2022).
53. He, Y., Liu, C., Yu, L. & Zhu, S. Enantio- and regioselective NiH-catalyzed reductive hydroarylation of vinylarenes with aryl iodides. *Angew. Chem. Int. Ed.* **59**, 21530–21534 (2020).
54. Yang, Z.-P. & Fu, G. C. Convergent catalytic asymmetric synthesis of esters of chiral dialkyl carbinols. *J. Am. Chem. Soc.* **142**, 5870–5875 (2020).
55. Jiang, X. et al. Nickel-catalyzed migratory hydroalkynylation and enantioselective hydroalkynylation of olefins with bromoalkynes. *Nat. Commun.* **12**, 3792 (2021).
56. Liu, J., Gong, H. & Zhu, S. Nickel-catalyzed, regio- and enantioselective benzylic alkenylation of olefins with alkenyl bromide. *Angew. Chem. Int. Ed.* **60**, 4060–4064 (2021).
57. Shi, L., Xing, L.-L., Hu, W.-B. & Shu, W. Regio- and enantioselective Ni-catalyzed formal hydroalkylation, hydrobenzylation, and

- hydropropargylation of acrylamides to  $\alpha$ -tertiary amides. *Angew. Chem. Int. Ed.* **60**, 1599–1604 (2021).
58. Sun, S.-Z. et al. Enantioselective deaminative alkylation of amino acid derivatives with unactivated olefins. *J. Am. Chem. Soc.* **144**, 1130–1137 (2022).
59. Cuesta-Galisteo, S., Schörghenheimer, J., Wei, X., Merino, E. & Nevado, C. Nickel-catalyzed asymmetric synthesis of  $\alpha$ -arylbenzamides. *Angew. Chem. Int. Ed.* **60**, 1605–1609 (2021).
60. Qian, D., Bera, S. & Hu, X. Chiral alkyl amine synthesis via catalytic enantioselective hydroalkylation of enecarbamates. *J. Am. Chem. Soc.* **143**, 1959–1967 (2021).
61. Wang, J.-W. et al. Catalytic asymmetric reductive hydroalkylation of enamides and enecarbamates to chiral aliphatic amines. *Nat. Commun.* **12**, 1313 (2021).
62. He, Y., Song, H., Chen, J. & Zhu, S. NiH-catalyzed asymmetric hydroarylation of N-acyl enamines to chiral benzylamines. *Nat. Commun.* **12**, 638 (2021).
63. Wang, S. et al. Enantioselective access to chiral aliphatic amines and alcohols via Ni-catalyzed hydroalkylations. *Nat. Commun.* **12**, 2771 (2021).
64. Maki, Y., Mori, H. & Endo, T. Xanthate-mediated controlled radical polymerization of N-vinylindole derivatives. *Macromolecules* **40**, 6119–6130 (2007).
65. Nakabayashi, K. & Mori, H. Recent progress in controlled radical polymerization of N-vinyl monomers. *Eur. Polym. J.* **49**, 2808–2838 (2013).
66. Rainka, M. P., Aye, Y. & Buchwald, S. L. Copper-catalyzed asymmetric conjugate reduction as a route to novel  $\beta$ -azaheterocyclic acid derivatives. *Proc. Natl Acad. Sci. USA* **101**, 5821–5823 (2004).
67. Sorensen, C. C. & Leibfarth, F. A. Stereoselective helix-sense-selective cationic polymerization of N-vinylcarbazole using chiral Lewis acid catalysis. *J. Am. Chem. Soc.* **144**, 8487–8492 (2022).
68. Wu, X., Ren, J., Shao, Z., Yang, X. & Qian, D. Transition-metal-catalyzed asymmetric couplings of  $\alpha$ -aminoalkyl fragments to access chiral alkylamines. *ACS Catal.* **11**, 6560–6577 (2021).
69. Rattanangkool, E., Vilaivan, T., Sukwattanasinitt, M. & Wacharasindhu, S. An atom-economic approach for vinylation of indoles and phenols using calcium carbide as acetylene surrogate. *Eur. J. Org. Chem.* **2016**, 4347–4353 (2016).
70. Kim, S. W., Schempp, T. T., Zbieg, J. R., Stivala, C. E. & Krische, M. J. Regio- and enantioselective iridium-catalyzed *n*-allylation of indoles and related azoles with racemic branched alkyl-substituted allylic acetates. *Angew. Chem. Int. Ed.* **58**, 7762–7766 (2019).
71. Sun, M., Liu, M. & Li, C. Rhodium-catalyzed chemodivergent regio- and enantioselective allylic alkylation of indoles. *Chem. Eur. J.* **27**, 3457–3462 (2021).
72. Cernak, T., Dykstra, K. D., Tyagarajan, S., Vachal, P. & Kraska, S. W. The medicinal chemist's toolbox for late stage functionalization of drug-like molecules. *Chem. Soc. Rev.* **45**, 546–576 (2016).
73. Lipshutz, B. H., Tomioka, T. & Pfeiffer, S. S. Mild and selective reductions of aryl halides catalyzed by low-valent nickel complexes. *Tetrahedron Lett.* **42**, 7737–7740 (2001).
74. Alonso, F., Beletskaya, I. P. & Yus, M. Metal-mediated reductive hydrodehalogenation of organic halides. *Chem. Rev.* **102**, 4009–4092 (2002).
75. Hammett, L. P. The effect of structure upon the reactions of organic compounds. benzene derivatives. *J. Am. Chem. Soc.* **59**, 96–103 (1937).
76. Hansch, C., Leo, A. & Taft, R. W. A survey of Hammett substituent constants and resonance and field parameters. *Chem. Rev.* **91**, 165–195 (1991).
77. Jensen, K. H. & Sigman, M. S. Evaluation of catalyst acidity and substrate electronic effects in a hydrogen bond-catalyzed enantioselective reaction. *J. Org. Chem.* **75**, 7194–7201 (2010).
78. Bandar, J. S., Pirnot, M. T. & Buchwald, S. L. Mechanistic studies lead to dramatically improved reaction conditions for the Cu-catalyzed asymmetric hydroamination of olefins. *J. Am. Chem. Soc.* **137**, 14812–14818 (2015).
79. Gutierrez, O., Tellis, J. C., Primer, D. N., Molander, G. A. & Kozlowski, M. C. Nickel-catalyzed cross-coupling of photoredox-generated radicals: uncovering a general manifold for stereoconvergence in nickel-catalyzed cross-couplings. *J. Am. Chem. Soc.* **137**, 4896–4899 (2015).

## Acknowledgements

We acknowledge the National Natural Science Foundation of China (Grant nos. 22101250, 22171240, 21861042), National Key R&D, Program of China (2019YFE0109200), Yunling Scholar of Yunnan Province, and Yunnan University (start-up grant to D.Q., CZ21623201) for financial support. We thank Advanced Analysis and Measurement Center of Yunnan University for the sample testing service.

## Author contributions

D.Q. directed the enantioselective synthesis of *N*-benzyl and *N*-allyl indoles; Z.S. directed the enantioselective synthesis of *N*-propargyl indoles; X.Y. directed some experiments on the enantioselective synthesis of *N*-benzyl indoles; L.L. and J.R. optimized the reaction conditions, conducted the control experiments, evaluated the scope of the reaction and applied this reaction to the diversification of the natural products and drugs; J.Z. and X.W. helped to evaluate the scope of the reaction; D.Q. wrote the manuscript.

## Competing interests

The authors declare no competing interest.

## Additional information

**Supplementary information** The online version contains supplementary material available at <https://doi.org/10.1038/s41467-022-34615-9>.

**Correspondence** and requests for materials should be addressed to Zhihui Shao, Xiaodong Yang or Deyun Qian.

**Peer review information** *Nature Communications* thanks the anonymous reviewers for their contribution to the peer review of this work.

**Reprints and permissions information** is available at <http://www.nature.com/reprints>

**Publisher's note** Springer Nature remains neutral with regard to jurisdictional claims in published maps and institutional affiliations.

**Open Access** This article is licensed under a Creative Commons Attribution 4.0 International License, which permits use, sharing, adaptation, distribution and reproduction in any medium or format, as long as you give appropriate credit to the original author(s) and the source, provide a link to the Creative Commons license, and indicate if changes were made. The images or other third party material in this article are included in the article's Creative Commons license, unless indicated otherwise in a credit line to the material. If material is not included in the article's Creative Commons license and your intended use is not permitted by statutory regulation or exceeds the permitted use, you will need to obtain permission directly from the copyright holder. To view a copy of this license, visit <http://creativecommons.org/licenses/by/4.0/>.

© The Author(s) 2022